Progress In Electromagnetics Research, Vol. 116, 425–439, 2011

EFFICIENT ANALYSIS OF SCATTERING FROM MULTIPLE 3-D CAVITIES BY MEANS OF A FE-BI-DDM METHOD

Z.-W. Cui*, **Y.-P. Han, C.-Y. Li, and W.-J. Zhao**

School of Science, Xidian University, No. 2 Taibai Road, Xian, Shaanxi, China

Abstract—A finite element-boundary integral-domain decomposition method is presented for analyzing electromagnetic scattering problems involving multiple three-dimensional cavities. Specifically, the edge-based finite element method is applied inside each cavity to derive a linear system of equations associated with unknown fields. The boundary integral equation is then applied on the apertures of all the cavities to truncate the computational domain and to connect the matrix subsystem generated from each cavity. With the help of an iterative domain decomposition method, the coupling system of equations is reduced to a small one which only includes the unknowns on the apertures. To further reduce computational burdens, the multilevel fast multipole algorithm is adopted to solve the reduced system. The numerical results for the near and far fields of several selected multi-cavity problems are presented to demonstrate the validity and capability of the proposed method.

1. INTRODUCTION

The electromagnetic characterization of cavities is important in many applications, such as radar cross section control, patch antenna design and surface defect detection. In recent years, there has been a growing interest in studying the scattering behavior of multiple cavities in conducting structures.

The problem of electromagnetic scattering by multiple two-dimensional (2-D) cavities in conducting plane has been considered by many authors. Kok [1] solved the problem using boundary value techniques in vector-field diffraction theories. Depine and Skigin [2]

Received 23 April 2011, Accepted 10 May 2011, Scheduled 16 May 2011

* Corresponding author: Zhiwei Cui (zwcui@mail.xidian.edu.cn).

developed a modal method for solving the problem. Reed and Byrne [3] later applied the modal method to analyze frequency-selective surfaces consisting of an array of multiple apertures within a periodic cell. Schiavone et al. [4] adopted the scattering patterns approach to investigate the electromagnetic scattering of multiple 2-D cavities recessed in a perfectly conducting plane. Recently, Alavikia and Ramahi [5] studied the problem of scattering from multiple 2-D cavities in a perfectly conducting plane by means of a novel finite element method (FEM) that uses the surface integral equation with the free-space Green's function as the boundary constraint. While much work has been done in the area of solving the problems of electromagnetic scattering by multiple 2-D cavities, little work on the solution of three dimensional (3-D) problems have been reported in the previous literature. The purpose of this work is to present a general, robust, and efficient approach for analyzing electromagnetic scattering from multiple 3-D cavities in conducting structures. In what follows, we first propose a powerful and versatile general numerical method for solving the problem of scattering by a 3-D single cavity. Then we extend the method to the case of multiple cavities.

Traditionally, the problem of scattering by a 3-D single cavity in a perfect conducting plane is solved by decoupling the fields inside the cavity from those outside by closing the aperture with a perfect conductor and introducing equivalent magnetic current over the over the extent of the aperture. The fields in the free space outside the cavity due to the equivalent magnetic currents can be easily formulated by using free-space Green's function. However, to explicitly express the fields inside the cavity in terms of the equivalent magnetic current, we require knowledge of the Green's function inside the cavity. For rectangular or circular cavities filled with homogeneous material, this is usually found in modal form [6, 7], but there is no available closed form of the associated Green's function for the case of arbitrarily shaped cavities. Although the methods based on integral equations [8–10] can be used to calculate the magnetic currents on the apertures of arbitrarily shaped cavities, it cannot be used when encountering cavities having inhomogeneous fillings. To overcome these difficulties, Jin and Volakis [11] employed the FEM to formulate the fields inside the cavity region. Specifically, the fields within the cavity, usually containing inhomogeneous materials, are modeled employing a finite element formulation, whereas the fields external to the cavity, filled with a homogeneous medium (most frequently, free space), are expressed by some sort of boundary integral equations (BIE) with free-space Green's function. The fields are then coupled across the aperture by means of the appropriate boundary conditions. Such hybrid method is commonly termed hybrid finite element-boundary integral (FE-BI) method [11–14], which has been widely proved to be a general, robust, and accurate numerical method for electromagnetic scattering from general-shape cavities with inhomogeneous fillings.

As is well-known, there is no direct coupling between the fields of any two independent FEM computational domains. Additionally, the Green's function relates the field at one point on the boundary to the fields at all other points of the boundary. Therefore, the hybrid FE-BI method is capable of being extended to the solution of electromagnetic scattering problems involving multiple cavities. This paper presents a domain decomposition of the hybrid FE-BI method to analyze scattering by multiple 3-D cavities. The idea of the method can be summarized as follows. The edge-based FEM is used to obtain the solution of vector wave equation inside each cavity. The BIE using the free-space Green's function is applied on the surfaces of the objects as a global boundary condition. To reduce computational burdens, the domain decomposition method (DDM) [15–17] in combination with the multilevel fast multipole algorithm (MLFMA) [18–23] is utilized to solve the coupling system of equations. In the following sections the theoretical and implementation of the proposed method are discussed in detail. The numerical results for the near and far fields of several selected multi-cavity problems are then presented to demonstrate the validity and capability of the proposed method.

2. FORMULATION

2.1. FE-BI Formulation for Scattering from a Single Cavity

As shown Figure 1, we first consider the problem of scattering by a 3-D single cavity in an infinite conducting plane. In accordance with the hybrid FE-BI method, the electric field inside the cavity and at

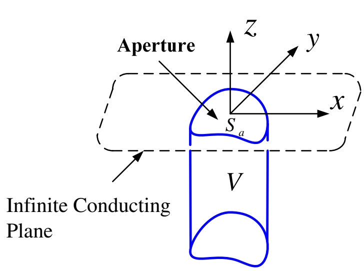

Figure 1. Geometry of a 3-D cavity in an infinite conducting plane.

the aperture of the cavity can be obtained by seeking the stationary point of the functional [24]

$$\begin{aligned} F(\mathbf{E}) = & \frac{1}{2}\iiint_V \left[\frac{1}{\mu_r}(\nabla\times\mathbf{E})\cdot(\nabla\times\mathbf{E}) - k_0^2\varepsilon_{\mathbf{r}}\mathbf{E}\cdot\mathbf{E}\right]dV \\ & -k_0^2\iint_{S_a}\mathbf{M}(\mathbf{r})\cdot\left[\iint_{S_a}\mathbf{M}(\mathbf{r}')\,G_0(\mathbf{r},\mathbf{r}')\,dS'\right]dS \\ & +\iint_{S_a}\nabla\cdot\mathbf{M}(\mathbf{r})\left[\iint_{S_a}G_0(\mathbf{r},\mathbf{r}')\,\nabla'\cdot\mathbf{M}(\mathbf{r}')\,dS'\right]dS \\ & +2jk_0Z_0\iint_{S_a}\mathbf{M}(\mathbf{r})\cdot\mathbf{H}^{inc}(\mathbf{r})\,dS. \end{aligned} \tag{1}$$

where V denotes the volume of the cavity, S_a denotes the area of the aperture and $\mathbf{H}^{inc}$ denotes the incident magnetic field. $\mathbf{M} = \mathbf{E}_S\times\hat{n}$ is the equivalent magnetic current over the aperture, in which $\mathbf{E}_S$ is the electric fields over the aperture and $\hat{n}$ is the outward unit vector normal to the aperture. Also, k_0, Z_0 and G_0 are the free-space wave number, wave impedance and scalar Green's function, respectively.

To discretize the functional F, the cavity volume is subdivided into a number of small tetrahedral elements. Consequently, the aperture of the cavity is divided into triangular elements. By using the Whitney vector basis functions defined on tetrahedral elements [24], the unknown electric field can be approximated as

$$\mathbf{E} = \sum_{j=1}^{N_V}\mathbf{N}_jE_j \tag{2}$$

where $\mathbf{N}_j$ denote the vector basis functions associated with the tetrahedral element edges, E_j denote the unknown expansion coefficients equal to the tangential electric fields at the tetrahedral element edges, and N_V denotes the total number of element edges resulting from the subdivision, including those on the aperture surface S_a. Accordingly, the magnetic current on the aperture can be expressed in terms of the unknown coefficients associated with the electric field as

$$\mathbf{M} = -\hat{n}\times\mathbf{E}_S = -\sum_{j=1}^{N_S}\mathbf{g}_jE_{S,j} \tag{3}$$

where N_S is the total number of triangular element edges on the aperture surface S_a, $\mathbf{g}_j$ are the Rao-Wilton-Glisson (RWG) [25] vector basis functions, which are completely compatible with the Whitney vector basis functions for the tetrahedral elements, i.e., $\mathbf{g}_j = \hat{n}\times N_j$, and $E_{S,j}$ are the unknown expansion coefficients on the aperture of the cavity.

Substituting (2) and (3) into (1) and performing the standard Rayleigh-Ritz procedure [24], we obtain a system of equations

$$\begin{bmatrix} K_{II} & K_{IS} \\ K_{SI} & K_{SS}+P \end{bmatrix} \begin{Bmatrix} E_I \\ E_S \end{Bmatrix} = \begin{Bmatrix} 0 \\ b \end{Bmatrix} \tag{4}$$

where $\{E_I\}$ denotes the unknowns in the interior cavity, $\{E_S\}$ denotes the unknowns on the aperture of the cavity, and $[K]$ that consists of $[K_{II}], [K_{IS}], [K_{SI}]$ and $[K_{SS}]$ is contributed by the volume integral in (1), whereas $[P]$ is contributed by the dual surface integral. The elements of matrices $[K]$ and $[P]$, and the vector $\{b\}$ are given by

$$K_{ij} = \iiint_V \left[\frac{1}{\mu_r}\{\nabla\times\mathbf{N}_i\}\cdot\{\nabla\times\mathbf{N}_j\} - k_0^2\varepsilon_r\{\mathbf{N}_i\}\cdot\{\mathbf{N}_j\}\right]dV \tag{5}$$

$$P_{ij} = -2k_0^2\iint_{S_a}\mathbf{g}_i(\mathbf{r})\cdot\left\{\iint_{S_a}\left[\mathbf{g}_j(\mathbf{r}')+\frac{1}{k_0^2}\nabla\nabla'\cdot\mathbf{g}_j(\mathbf{r}')\right]G_0(\mathbf{r},\mathbf{r}')dS'\right\}dS \tag{6}$$

$$b_i = -2jk_0Z_0\iint_{S_a}\mathbf{g}_i\cdot\mathbf{H}^{inc}dS \tag{7}$$

For the sake of clear description, we define an integral operator

$$L(\mathbf{g}_j) = -2k_0^2\iint_{S_a}\left[\mathbf{g}_j(\mathbf{r}')+\frac{1}{k_0^2}\nabla\nabla'\cdot\mathbf{g}_j(\mathbf{r}')\right]G_0(\mathbf{r},\mathbf{r}')\,dS' \tag{8}$$

With the integral operator, the elements of matrix $[P]$ can be expressed as

$$P_{ij} = \iint_{S_a}\mathbf{g}_i\cdot L(\mathbf{g}_j)\,dS \tag{9}$$

where $\mathbf{g}_i$ and $\mathbf{g}_j$ denote the testing and expansion basis functions, respectively. In this notation, the testing and expansion locations are both on the aperture of the same cavity.

2.2. Extension to Multiple Cavities

To extend the method described above to case of multiple cavities, we propose an expanded system of equations with individual $[P]$ sub-matrices. The new $[P]$ sub-matrices take on the form

$$[P_{ij}]^{mn} = \iint_S \mathbf{g}_i^m\cdot L_{mn}\left(\mathbf{g}_j^n\right)dS \tag{10}$$

The new integral operators L_{mn} is defined as

$$L_{mn}\left(\mathbf{g}_j^n\right) = -2k_0^2\iint_S\left[\mathbf{g}_j^n(\mathbf{r}')+\frac{1}{k_0^2}\nabla\nabla'\cdot\mathbf{g}_j^n(\mathbf{r}')\right]G_0(\mathbf{r},\mathbf{r}')\,dS' \tag{11}$$

where the subscript "S" represents the surface integration in (11) is performed over the apertures of all the cavities, and the indices $[m, n]$ represent the testing and expansion cavities, respectively. Thus, the notation $\left[P^{11}\right]$ implies that the testing and expansion locations are both on the aperture of the cavity 1, whereas $\left[P^{12}\right]$ indicates that the testing locations are on the aperture of the cavity 1, but the expansion locations are on the aperture of the cavity 2.

According to the principle of FEM, there is no direct coupling between the unknowns of any two independent cavities. Therefore, the FEM matrix $[K]$ is only defined when $m = n$. In other words, the cavities are coupled to each other only through the surface integral equation based on the Green's function. Without loss of generality, we consider the scattering problem for two cavities in an infinite conducting plane, as shown in Figure 2. If the unknowns on the apertures are numbered last, the coupling system of equations can be expressed as

$$\begin{bmatrix} K_{II}^1 & 0 & K_{IS}^1 & 0 \\ 0 & K_{II}^2 & 0 & K_{IS}^2 \\ K_{SI}^1 & 0 & K_{SS}^1 + P^{11} & P^{12} \\ 0 & K_{SI}^2 & P^{21} & K_{SS}^2 + P^{22} \end{bmatrix} \begin{Bmatrix} E_I^1 \\ E_I^2 \\ E_S^1 \\ E_S^2 \end{Bmatrix} = \begin{Bmatrix} 0 \\ 0 \\ b^1 \\ b^2 \end{Bmatrix} \tag{12}$$

Generalizing the formulation to m cavities results in the following equation system

$$\begin{bmatrix} \widetilde{K}_{II} & \widetilde{K}_{IS} \\ \widetilde{K}_{SI} & \widetilde{K}_{SS} + \widetilde{P} \end{bmatrix} \begin{Bmatrix} \widetilde{E}_I \\ \widetilde{E}_S \end{Bmatrix} = \begin{Bmatrix} 0 \\ \widetilde{b} \end{Bmatrix} \tag{13}$$

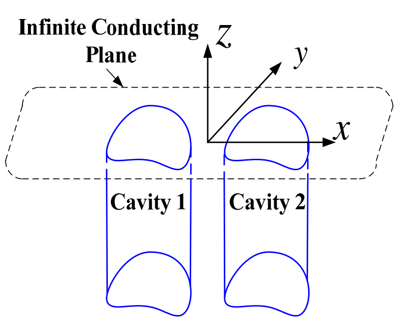

Figure 2. Geometry of two 3-D cavities in a conducting plane.

where

$$\left[\widetilde{K}_{II}\right]=\begin{bmatrix} K_{II}^1 & & & \\ & K_{II}^2 & & \\ & & \ddots & \\ & & & K_{II}^m \end{bmatrix}, \quad \left[\widetilde{K}_{IS}\right]=\begin{bmatrix} K_{IS}^1 & & & \\ & K_{IS}^2 & & \\ & & \ddots & \\ & & & K_{IS}^m \end{bmatrix},$$

$$\left[\widetilde{K}_{SI}\right]=\begin{bmatrix} K_{SI}^1 & & & \\ & K_{SI}^2 & & \\ & & \ddots & \\ & & & K_{SI}^m \end{bmatrix}, \quad \left[\widetilde{K}_{SS}\right]=\begin{bmatrix} K_{SS}^1 & & & \\ & K_{SS}^2 & & \\ & & \ddots & \\ & & & K_{SS}^m \end{bmatrix} \tag{14}$$

$$\left[\widetilde{P}\right]=\begin{bmatrix} P^{11} & P^{12} & \dots & P^{1m} \\ P^{21} & P^{22} & \dots & P^{2m} \\ \vdots & \vdots & \ddots & \vdots \\ P^{m1} & P^{m2} & \dots & P^{mm} \end{bmatrix} \tag{15}$$

$$\left\{\widetilde{E}_I\right\} = \begin{Bmatrix} E_I^1 \\ E_I^2 \\ \vdots \\ E_I^m \end{Bmatrix}, \quad \left\{\widetilde{E}_S\right\} = \begin{Bmatrix} E_S^1 \\ E_S^2 \\ \vdots \\ E_S^m \end{Bmatrix}, \quad \left\{\widetilde{b}\right\} = \begin{Bmatrix} b^1 \\ b^2 \\ \vdots \\ b^m \end{Bmatrix} \tag{16}$$

2.3. Iterative Domain Decomposition Solver

To efficiently solve Equation (13), we develop a hybrid domain decomposition algorithm based on the iterative substructuring method [15] and the MLFMA In the implementation of the algorithm, we first eliminate the unknowns in the interior of each cavity according to the following equation

$$\left\{E_I^i\right\} = -\left[K_{II}^i\right]^{-1}\left[K_{IS}^i\right]\left\{E_S^i\right\} \quad (i = 1, 2, \dots, m) \tag{17}$$

Once all the interior unknowns are eliminated, the original equation system is reduced to a small one which only includes the unknowns on the apertures of the cavities, as follows

$$\left[S+\widetilde{P}\right]\left\{\widetilde{E}_S\right\} = \left\{\widetilde{b}\right\} \tag{18}$$

where

$$[S] = \begin{bmatrix} S^1 & & & \\ & S^2 & & \\ & & \ddots & \\ & & & S^m \end{bmatrix} \tag{19}$$

$$\left[S^i\right] = \left[K_{SS}^i\right] - \left[K_{SI}^i\right]\left[K_{II}^i\right]^{-1}\left[K_{IS}^i\right] \tag{20}$$

The computation (20) can be performed with the following procedure

$$\left[K_{II}^{i}\right] = [L]\,[U] \tag{21}$$

$$[M] = [L]^{-1}\left[K_{IS}^{i}\right] \tag{22}$$

$$\left[S^{i}\right] = \left[K_{SS}^{i}\right] - [U]^{-1}\,[M] \tag{23}$$

where $[L]$ is the lower triangular matrix and $[U]$ is the upper triangular matrix. To reduce the memory requirement, we employ the multifrontal method [26, 27] to factorize the matrix $\left[K_{II}^{i}\right]$. The multifrontal method is an advanced version of the frontal method proposed by Irons [28], which partitions the whole factorization process into the factorization of a number of small dense frontal matrices [29]. During factorization, only the frontal matrix remains in the core memory. The factorized equations are stored in the out-of-core memory. Through this strategy, the memory needed can be reduced to minimal.

Before further proceeding, it should be noted that the computation from (21) to (23) in each cavity is independent, and can be completely parallelized. Furthermore, all the cavities can be classified into a few building blocks according to the geometrical features, in such a manner only $\left[S^{i}\right]$ for different types of cavities need to be evaluated rather than all the cavities. If the cavities are all the same, only one sub-matrix $\left[S^{i}\right]$ needs to be evaluated to assemble the global matrix $[S]$.

Usually, the reduced system (18) can be solved by an iterative solver such as the generalized minimum residual (GMRES) method [30]. However, traditional GMRES iteration method incurs very high computational cost and memory requirements with the increasing of the unknowns. In addition, the conventional approaches to computing the BIE matrix elements consume a considerable portion of the total solution time, and this, in turn, can place an inordinately heavy burden on the CPU regarding memory and time. To overcome these difficulties, we employ the MLFMA to the BIE matrix to significantly reduce the memory requirement and computational complexity. The detailed description of MLFMA is given in [18] and is not repeated here.

3. NUMERICAL RESULTS

Once the unknown coefficients for the electric fields at the apertures are solved from (18), the magnetic currents at the apertures and the scattered field in the free space region above the conducting plane can be computed. The near-zone scattered fields can be calculated from

$$\mathbf{E}_{near}^{sca}(\mathbf{r}) = -2 \iint_S \mathbf{M}(\mathbf{r}') \times \nabla' G_0(\mathbf{r}, \mathbf{r}')\, dS' \quad (24)$$

$$\mathbf{H}_{near}^{sca}(\mathbf{r}) = -2jk_0 \frac{1}{Z_0} \iint_S \left[\mathbf{M}(\mathbf{r}') + \frac{1}{k_0^2} \nabla\nabla' \cdot \mathbf{M}(\mathbf{r}')\right] G_0(\mathbf{r}, \mathbf{r}')\, dS' \quad (25)$$

where the surface integration in (24) and (25) is performed over the apertures of all cavities. In the far-field region, the free-space scalar Green's function can be approximated by

$$G_0(\mathbf{r}, \mathbf{r}') \cong \frac{e^{-jk_0 r}}{4\pi r} e^{jk_0 \mathbf{r}' \cdot \hat{\mathbf{r}}} \quad (26)$$

Substituting (26) back into (24) and (25), the far-zone scattered fields can be expressed as

$$\mathbf{E}_{far}^{sca}(\mathbf{r}) \cong 2jk_0 \frac{e^{-jk_0 r}}{4\pi r} \iint_S \hat{\mathbf{r}} \times \mathbf{M}(\mathbf{r}') e^{jk_0 \mathbf{r}' \cdot \hat{\mathbf{r}}} dS' \quad (27)$$

$$\mathbf{H}_{far}^{sca}(\mathbf{r}) \cong 2jk_0 \frac{1}{Z_0} \frac{e^{-jk_0 r}}{4\pi r} \iint_S \hat{\mathbf{r}} \times \left[\hat{\mathbf{r}} \times \mathbf{M}(\mathbf{r}')\right] e^{jk_0 \mathbf{r}' \cdot \hat{\mathbf{r}}} dS' \quad (28)$$

In what follows, we present some numerical results to demonstrate the validity and capability of the proposed hybrid FE-BI-DDM technique. The results to be presented are in terms of magnitude and scattering cross section. The magnitude of the scattered field in the near-field region is defined by

$$\psi = \left|\mathbf{E}_{near}^{sca}\right| \quad \text{or} \quad \psi = \left|\mathbf{H}_{near}^{sca}\right| \quad (29)$$

The scattering cross section in the far-field region is defined as

$$\sigma = \lim_{r\to\infty} 4\pi r^2 \frac{\left|\mathbf{E}_{far}^{sca}\right|^2}{\left|\mathbf{E}^{inc}\right|^2} = \lim_{r\to\infty} 4\pi r^2 \frac{\left|\mathbf{H}_{far}^{sca}\right|^2}{\left|\mathbf{H}^{inc}\right|^2} \quad (30)$$

Without loss of generality, the magnitude of the incident electric field is assumed to be unity throughout this work. To discretize the solution domain, we use first-order tetrahedral elements with mesh density of approximately 12 parts per wavelength. All calculations are carried out on a personal computer with 3.0 GHz CPU and 4 GB memory. Here the GMRES iteration method with a relative error norm of 0.001 is adopted.

The first example considered is the scattering by two identical rectangular cavities in a conducting plane. Both cavities are rectangular with dimension of $1.0\lambda \times 1.0\lambda \times 0.5\lambda$ and are separated by distances of 0.5λ in x-direction, λ being the operating wavelength. The

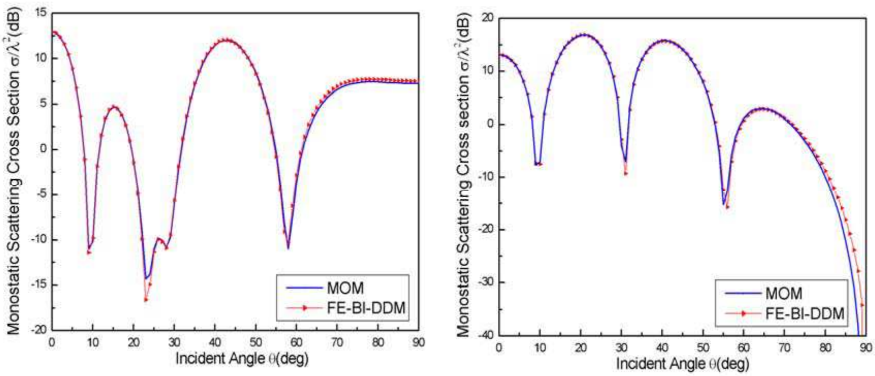

(a) (b)

Figure 3. Monostatic scattering cross section of two identical $1.0\lambda \times 1.0\lambda \times 0.5\lambda$ rectangular cavities: (a) $\theta\theta$ polarization; (b) $\varphi\varphi$ polarization.

monostatic scattering cross section computed by the proposed method are plotted in Figure 3, and compared with those from the method of moments (MOM) based on the surface boundary integral equation. As is evident from the figure, good agreement is obtained between the two methods. This demonstrates the validity of the FE-BI-DDM method In this example, each cavity is discretized independently into 3485 tetrahedral elements. As a result, a total of 7420 FEM unknowns and 626 BIE unknowns are generated. Although the number of unknowns is large, the memory needed can be reduced to minimal by virtue of the iterative domain decomposition solver described in Section 2.3. For the problem considered here, the memory required is only about 9 MB.

In the second example, we investigate the scattering behavior of four identical $2.0\lambda \times 2.0\lambda \times 3.0\lambda$ rectangular cavities recessed in a conducting plane. The cavities are arranged in three ways and are separated by distances of 0.5λ. In the first, the cavities are placed along y-axis. In the second, the cavities are placed along x-axis. In the last, the cavities are arranged periodically in both the x and y directions, i.e., a 2×2 array. Figure 4 depicts the computed scattering cross section as a function of the angle of incidence in the xoz plane. As can be seen, when the cavities are placed along y-axis, the scattering cross section curve in the xoz plane is relatively smooth, whereas the curves corresponding to the other two ways have several peaks. This indicates that the coupling effects among the cavities are stronger in the last two ways than that in the first one. Furthermore, we can observe that the locations and the values of the peaks in the last two

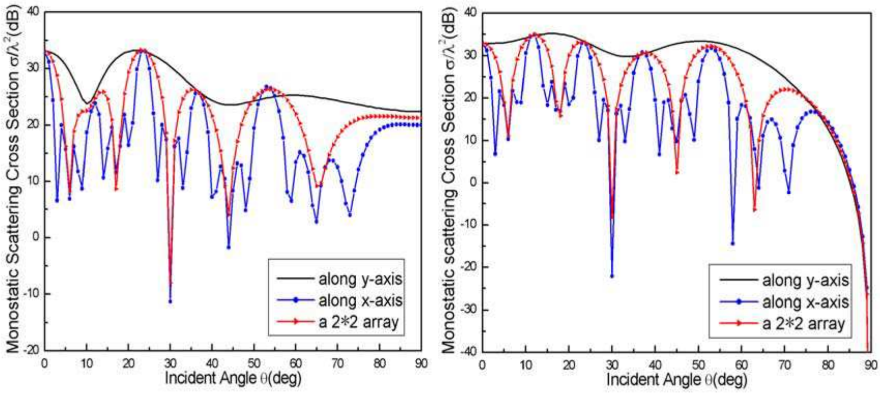

(a) (b)

Figure 4. Monostatic scattering cross section of four identical $2.0\lambda \times 2.0\lambda \times 3.0\lambda$ rectangular cavities: (a) $\theta\theta$ polarization; (b) $\varphi\varphi$ polarization.

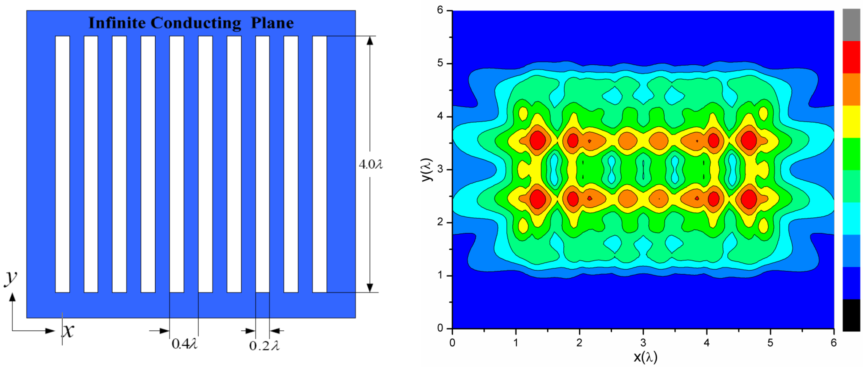

(a) (b)

Figure 5. Ten long and narrow rectangular cavities embedded in an infinite conducting plane: (a) geometrical configuration; (b) magnitude of electric field.

curves are the same.

The third example to consider is the scattering of a plane wave from ten long and narrow rectangular cavities embedded in an infinite conducting plane, as shown in Figure 5(a). All these cavities are assumed to be identical with a rectangular $0.2\lambda \times 4.0\lambda$ aperture and a depth 0.6λ. The cavities are arranged periodically with a spacing of 0.2λ in the x-direction. The plane wave with the electric field parallel

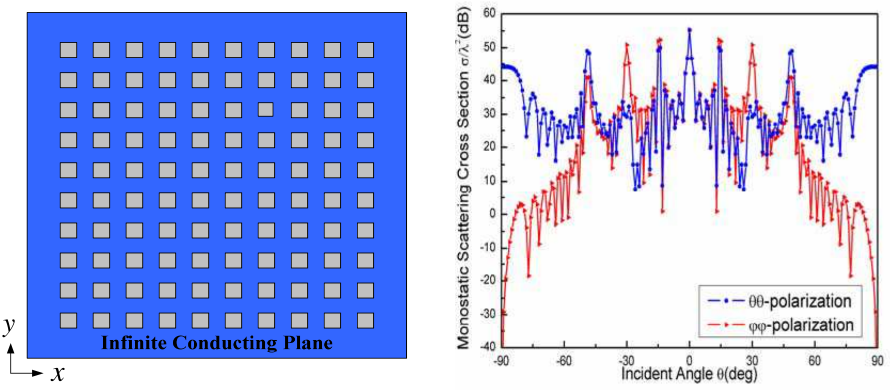

(a) (b)

Figure 6. A 10×10 array of rectangular cavities: (a) geometrical configuration; (b) monostatic scattering cross section.

to the x-axis is incident in the normal direction. Figure 5(b) shows the magnitude of electric field calculated at a plane located at a distance of $z = 0.2\lambda$ above the apertures.

The final example used to demonstrate the capability of the proposed method is a 10×10 cavity array depicted in Figure 6(a). Each cavity of the array has a square $1.0\lambda \times 1.0\lambda$ aperture and is 0.6λ deep. Periodicities in both x and y directions of the array are 2.0λ. The cavities are assumed to be filled with lossy dielectric having $\varepsilon_r = 2.0 - j2.0$ and $\mu_r = 1.0$. For numerical solution, a total of 418200 tetrahedral elements are used to discretize the array cavities, which result in 1012700 FEM unknowns and 61700 BIE unknowns Although the number of FEM unknowns is very large, only one percent of those need to be dealt with. Furthermore, the reduced full system can be converted into a sparse one by virtue of MLFMA. In this problem, 5-level MLFMA is used, and the memory required is about 850 MB. The computed scattering cross section is given in Figure 6(b) as a function of the angle of incidence.

4. CONCLUSION

In this paper, the FE-BI method was extended to analyze electromagnetic scattering from multiple 3-D cavities in an infinite perfectly conducting plane. To reduce the computational burdens of the method, an iterative substructuring method was employed to solve the coupling system of equations. As a result, the original problem was reduced to a small one which only includes the unknowns on the apertures. Furthermore, the reduced system was solved by the GMRES method, where the MLFMA can be employed to reduce the memory requirement and computational complexity. Some of our preliminary numerical results are presented to illustrate the validity and capability of the proposed method on dealing with multi-cavity problems. In the future, we will extend the method to solution of the electromagnetic scattering problems involving multiple 3-D holes.

ACKNOWLEDGMENT

This work was supported by the National Natural Science Foundation of China (Grant No. 60771039) and the Fundamental Research Funds for the Central Universities (Grant No. k50510070011).

REFERENCES

1. Kok, Y. L., "General solution to the multiple-metallic-grooves scattering problem: The fast-polarization case," *Applied Opt.*, Vol. 32, No. 14, 2573–2581, 1993.
2. Depine, R. A. and D. C. Skigin, "Scattering from metallic surfaces having a finite number of rectangular grooves," *J. Opt. Soc. Am. A*, Vol. 11, No. 11, 2844–2850, 1994.
3. Reed, J. A. and D. M. Byrne, "Frequency-selective surfaces with multiple apertures within a periodic cell," *J. Opt. Soc. Am. A*, Vol. 15, No. 3, 660–668, 1998.
4. Schiavone, G. A., K. O'Neill, and K. D. Paulsen, "Scattering from groove patterns in a perfectly conducting surface," *J. Opt. Soc. Am. A*, Vol. 14, No. 9, 660–668, 1997.
5. Alavikia, B. and O. M. Ramahi, "Finite-element solution of the problem of scattering from cavities in metallic screens using the surface integral equation as a boundary constraint," *J. Opt. Soc. Am. A*, Vol. 26, No. 9, 1915–1925, 2009.
6. Altintas, A., P. H. Pathak, and M. C. Liang, "A selective modal scheme for the analysis of EM coupling into or radiation from large open-ended waveguide," *IEEE Trans. Antennas Propagat.*, Vol. 36, No. 1, 84–96, 1988.
7. Anastassiu, H. T., J. L. Volakis, and D. C. Ross, "The mode matching technique for electromagnetic scattering by cylindrical waveguides with canonical terminations," *Journal of Electromagnetic Waves and Applications*, Vol. 9, No. 11–12, 1363–1391, 1995.
8. Wang, T., R. F. Harrington, and J. R. Mautz, "Electromagnetic scattering and transmission through arbitrary apertures in

conducting bodies," *IEEE Trans. Antennas Propagat.*, Vol. 38, No. 1, 1805–1814, 1990.

9. Barkeshli, K. and J. L. Volakis, "Electromagnetic scattering from an aperture formed by a rectangular cavity recessed in a ground plane," *Journal of Electromagnetic Waves and Applications*, Vol. 5, No. 7, 715–734, 1991.
10. Wang, T. M. and H. Ling, "Electromagnetic scattering from three- dimensional cavities via a connection scheme," *IEEE Trans. Antennas Propagat.*, Vol. 39, No. 10, 1505–1513, Oct. 1991.
11. Jin, J. M. and J. L. Volakis, "A finite element-boundary integral formulation for scattering by three-dimensional cavity-backed apertures," *IEEE Trans. Antennas Propagat.*, Vol. 39, No. 1, 97–104, Jan. 1991.
12. Hua, Y. and J. Li, "Analysis of longitudinal shunt waveguide slots using FE-BI," *Journal of Electromagnetic Waves and Applications*, Vol. 23, No. 14–15, 2041–2046, 2009.
13. Yang, M. L. and X. Q. Sheng, "Parallel high-order FE-BI-MLFMA for scattering by large and deep coated cavities loaded with obstacles," *Journal of Electromagnetic Waves and Applications*, Vol. 23, No. 13, 1813–1823, 2009.
14. Peng, Z., X.-Q. Sheng, and F. Yin, "An efficient twofold iterative algorithm of FE-BI-MLFMA using multilevel inverse-based ILU preconditioning," *Progress In Electromagnetics Research*, Vol. 93, 369–384, 2009.
15. Toselli, A. and O. Widlund, *Domain Decomposition Methods — Algorithms and Theory*, Springer, Berlin, 2005.
16. Cui, Z. W. and Y. P. Han, "The substructure method for scattering by large open-ended cavities," *Chinese Journal of Radio Science*, Vol. 24, No. 5, 914–919, Oct. 2009.
17. Martini, E., G. Carli, and S. Maci, "A domain decomposition method based on a generalized scattering matrix formalism and a complex source expansion," *Progress In Electromagnetics Research B*, Vol. 19, 445–473, 2010.
18. Song, J. M., C. C. Lu, and W. C. Chew, "Multilevel fast multipole algorithm for electromagnetic scattering by large complex objects," *IEEE Trans. Antennas Propagat.*, Vol. 45, No. 10, 1488–1493, 1997.
19. Gürel, L., O. Ergül, A. Ünal, and T. Malas, "Fast and accurate analysis of large metamaterial structures using the multilevel fast multipole algorithm," *Progress In Electromagnetics Research*, Vol. 95, 179–198, 2009.

20. Taboada, J. M., M. G. Araújo, J. M. Bértolo, L. Landesa, F. Obelleiro, and J. L. Rodriguez, "MLFMA-FFT parallel algorithm for the solution of large-scale problems in electromagnetics," *Progress In Electromagnetics Research*, Vol. 105, 15–30, 2010.
21. Ergül, O., T. Malas, and L. Gürel, "Solutions of large-scale electromagnetics problems using an iterative inner-outer scheme with ordinary and approximate multilevel fast multipole algorithms," *Progress In Electromagnetics Research*, Vol. 106, 203–223, 2010.
22. Ergül, O. and L. Gürel, "Efficient solutions of metamaterial problems using a low-frequency multilevel fast multipole algorithm," *Progress In Electromagnetics Research*, Vol. 108, 81–99, 2010.
23. Shao, H., J. Hu, Z.-P. Nie, G. Han, and S. He, "Hybrid tangential equivalence principle algorithm with MLFMA for analysis of array structures," *Progress In Electromagnetics Research*, Vol. 113, 127–141, 2011.
24. Jin, J. M., *The Finite Element Method in Electromagnetics*, 2nd edition, Wiley, New York, 2002.
25. Rao, S. M., D. R. Wilton, and A. W. Glisson, "Electromagnetic scattering by surfaces of arbitrary shape," *IEEE Trans. Antennas Propagat.*, Vol. 30, No. 3, 409–418, 1982.
26. Liu, J. W. H., "The multifrontal method for sparse matrix solution: Theory and practice," *SIAM Rev.*, Vol. 34, 82–109, 1992.
27. Tian, J., Z.-Q. Lv, X.-W. Shi, L. Xu, and F. Wei, "An efficient approach for multifrontal algorithm to solve non-positive-definite finite element equations in electromagnetics problems," *Progress In Electromagnetics Research*, Vol. 95, 121–133, 2009.
28. Irons, B. M., "A frontal solution program for finite element analysis," *SIAM Rev.*, Vol. 2, 5–32, 1970.
29. Ping, X. W., T. J. Cui, and W. B. Lu, "The combination of bcgstab with multifrontal algorithm to solve FE-BI-MLFMA linear systems arising from inhomogeneous electromagnetic scattering problems," *Progress In Electromagnetics Research*, Vol. 93, 91–105, 2009.
30. Ergül, O. and L. Gürel, "Improving iterative solutions of the electricfield integral equation via transformations into normal equations," *Journal of Electromagnetic Waves and Applications*, Vol. 24, No. 16, 2129–2138, 2010.